Eur. Phys. J. Appl. Phys. **36**, 177–182 (2006)
DOI: 10.1051/epjap:2006116

THE EUROPEAN PHYSICAL JOURNAL
APPLIED PHYSICS

A technique for evaluating the RF voltage across the electrodes of a capacitively-coupled plasma reactor

V. Lisovskiy[1,3,a], J.-P. Booth[1], K. Landry[2], D. Douai[2], V. Cassagne[2], and V. Yegorenkov[3]

[1] Laboratoire de Physique et Technologie des Plasmas, École Polytechnique, 91128 Palaiseau, France
[2] Unaxis Displays Division France SAS, 5, rue Leon Blum, 91120 Palaiseau, France
[3] Department of Physics and Technology, Kharkov National University, Kharkov 61077, Ukraine

Received: 26 June 2006 / Received in final from: 28 July 2006 / Accepted: 28 July 2006
Published online: 11 October 2006 –

Abstract. We propose a new technique for evaluating the RF voltage across the electrodes of low-pressure capacitively-coupled plasma reactors when direct measurements are not possible. It is based on determining the coordinates of the turning point in the RF breakdown curve and using known values of the electron drift velocity for the gas. The results are in good agreement with those obtained by direct measurements at the driven electrode. Furthermore it allows RF breakdown curves to be determined for different frequencies, giving results that are physically reasonable (coincidence of right-hand branches) and in agreement with other published results. The technique for determining RF voltage we proposed is valid when there is no discharge plasma between electrodes (e.g., before gas breakdown), as well as for negligibly small discharge currents (before extinction of the weak-current discharge mode).

PACS. 52.80.Pi High-frequency and RF discharges – 52.20.Fs Electron collisions

1 Introduction

Low-pressure capacitive RF discharges are widely used for technological surface treatment processes, including deposition of films on the surface of various materials (PECVD), etching of semiconductor wafers, plasma sterilization of medical tools and materials etc. The plasma reactors used generally contain planar electrodes placed inside a larger grounded vessel. In large industrial devices is often difficult to access the powered electrode surface to measure the true RF voltage. Therefore different equivalent circuits models have been used to describing the reactor impedance, allowing the magnitude of the RF voltage to be estimated (see, for example, [1–4]). A number of assumptions must be made concerning the structure of the equivalent circuit, in order to estimate the inductances L, resistances R and capacitances C of the constituent elements. Obviously the precision of this method will strongly depend on the correctness of these assumptions.

Miller [5,6] and Sobolewski [7,8] made large contributions to the development of correct methods of rf measurements. They proposed to include an external inductive shunt into the electric circuit, which tuning can compensate rf displacement current. At the same time rf discharge current and impedance can be correctly estimated. However, as we see from Table II [7], application of a shunt did not lead to a noticeable improvement of the accuracy of RF voltage measurement at the driven electrode (with the rf voltage at the driven electrode of ≈ 118 V the rf voltage probe determined the voltage value as 98.6 V without the shunt and 97.2 V with the shunt).

Therefore for estimating the rf voltage at driven electrode it is desirable to employ an auxiliary technique which depended only on the parameters of the rf discharge gap (rf voltage, gas pressure, discharge gap) but not on the parameters of the external circuit. Even if this technique permits to estimate the value of the rf voltage at driven electrode at certain conditions (e.g., without discharge within the gap), it will help to draw a conclusion on the correctness of measurements with the inductive shunt.

The authors of papers [9–15] proposed a novel method for determining the electron drift velocity V_{dr} in a gas, as a function of the reduced electric field, from the location of the low-pressure turning point in the breakdown curve of a low-pressure RF capacitive discharge. This method allows V_{dr} to be determined for high electric fields, where other conventional techniques become difficult. The values obtained by this method are in good agreement with direct measurements of the electron drift velocity as well as with calculated data.

In this paper we propose a new technique for determining the magnitude of the RF potential at the driven electrode of a capacitive discharge when this is inaccessible to direct measurements. The technique is based on

[a] e-mail: lisovskiy@yahoo.com

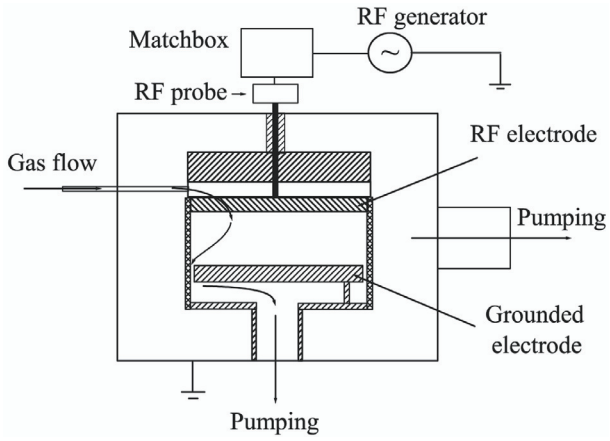

Fig. 1. Schematic of the experimental set-up.

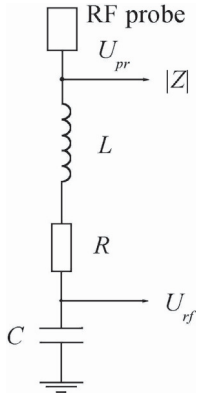

Fig. 2. Equivalent circuit of our chamber.

recording the breakdown curve of a low-pressure RF capacitive discharge and using a gas for which the electron drift velocity is well-known. The values of the RF voltage obtained in this way agree with direct measurements, and they are reasonable from the physical point of view. This technique permits to estimate the value of rf voltage at the driven electrode in the case of a negligibly small active discharge current (without discharge, before breakdown, as well as before discharge extinction).

2 Experimental device

In our experiments capacitive rf discharges were ignited in various gases over the pressure range $p \approx 0.01$–30 torr, with inter-electrode gaps of $d = 5$–27 mm and with RF frequencies of $f = 13.56$ MHz and $f = 27.12$ MHz. For brevity we present only the results obtained for N_2 though we tested the validity of the techniques also in Ar, He, H_2, NH_3, O_2, N_2O, SF_6, NF_3 and for mixtures of these gases. Some results for other gases were published in [14]. The planar circular aluminium electrodes were of 143 mm in diameter. The electrodes were located inside a fused silica tube with the inner diameter of 145 mm. The gas under study was fed through small orifices in the upper electrode and evacuated via a gap between the second electrode and the wall of the fused silica tube. This discharge chamber was surrounded with a grounded metal grid and contained in a larger grounded vessel 315 mm in diameter and 231 mm high (see Fig. 1). Breakdown in the larger vessel was prevented by the grounded grid, the fused silica tube around the electrodes and the gas lower pressure outside the discharge chamber. The gas pressure was monitored with 10 and 1000 torr capacitive manometers (MKS Instruments). The gas flow was set with a mass flow controller to 1–5 sccm, and the pressure was regulated by throttling the outlet to the pump.

The rf voltage, with an amplitude of $U_{rf} < 1300$ V, was applied through a matchbox to the upper electrode, and the lower one was grounded. The rf voltage was fed to the driven electrode through a coaxial cable inside the larger vessel and connected to a feed-through mounted in its roof. The rf voltage U_{rf} was measured with an rf V-I probe (Advanced Energy Z'SCAN). This rf probe was located at the shortest possible distance from the rf electrode. The power was supplied by an rf generator (RF Power Products Inc. RF5S) via an L-type matchbox (Huttinger Elektronik Gmbh PFM). The impedance Z and the phase shift angle φ were determined using a Vector Impedance Meter (Hewlett Packard 4193A).

We used the technique proposed by Levitskii [16] to measure the rf breakdown curves. Near to, and to the high-pressure side of, the breakdown curve minimum the gas pressure was fixed before slowly increasing the rf voltage until gas breakdown occurs. To the low pressure side of the minimum the curve may be multi-valued, i.e. the curve turns back towards high pressure and breakdown occurs at two different values of the rf voltage. Therefore in this range we first decreased the gas pressure, then fixed the rf voltage value and only then increased the gas pressure slowly until discharge ignition occurred. At the moment of discharge ignition the rf voltage shows a sharp decrease, and a glow appears between the electrodes serving as our criterion for the onset of gas breakdown.

3 Equivalent circuit model of the discharge vessel

The RF potential at the driven electrode was estimated using the equivalent circuit shown in Figure 2. The feed-through and the coaxial cable were described by an inductance L and a resistance R, and the parallel electrodes (without discharge) as a capacitance C. The squared impedance modulus of such equivalent circuit, $|Z|^2$, for the frequency $\omega = 2\pi f$, is equal to

$$|Z|^2 = R^2 + \left(\omega L - \frac{1}{\omega C}\right)^2. \quad (1)$$

The value of $|Z|$ is measured at two frequencies: $|Z|$ at the frequency $f = 27.12$ MHz (for which we wish to determine the RF voltage) and $|Z|_{res}$ at the resonant frequency f_{res} for the given geometry of the discharge vessel. The resonant frequency is defined to be when the phase angle

$\varphi = 0$, then $|Z|_{res} = R$. Therefore we have

$$|Z|^2 = |Z|^2_{res} + \left(\omega L - \frac{1}{\omega C}\right)^2. \quad (2)$$

Taking into account that

$$f_{res} = \frac{1}{2\pi\sqrt{LC}}, \quad (3)$$

then we obtain:

$$C = \frac{\left|\frac{f^2}{f^2_{res}} - 1\right|}{2\pi f\sqrt{|Z|^2 - |Z|^2_{res}}}, \quad (4)$$

$$L = \frac{1}{C}\cdot\frac{1}{(2\pi)^2 f^2_{res}}, \quad (5)$$

$$U_{rf} = \frac{\sqrt{|Z|^2 - |Z|^2_{res}}}{\left|\frac{f^2}{f^2_{res}} - 1\right|\cdot|Z|}\cdot U_{pr}. \quad (6)$$

Here U_{rf} is the true RF voltage across the electrodes and U_{pr} is the rf voltage measured at the RF probe external to the reactor. Our aim is to relate the external voltage to the internal voltage.

Let us now discuss how to evaluate the magnitude of the rf potential at the driven electrode located inside a grounded vessel of large size. To this end it is usually necessary: (i) to connect an rf probe directly to the driven electrode (without the intermediate feedthrough and the connection cables), (ii) to have another rf probe at the feed-through (because the presence of an RF probe inevitably changes the system impedance). These conditions are not easily fulfilled because usually the driven electrode is inaccessible.

For relatively low frequencies (f = 13.56 MHz and lower) the voltage at the electrode will be close to the value measured by the external rf probe. However, at higher frequencies the rf probe will give incorrect values. The error is especially large when the required frequency, say, f = 27.12 MHz, is close to the natural resonant frequency of the discharge vessel, f_{res}.

This is the case for our discharge vessel. Figure 3 shows the impedance modulus $|Z|$ and the phase angle, φ, against frequency, f, measured with the Vector Impedance Meter. The resonance frequency, at which $\varphi = 0$, is equal to f_{res} = 33.14 MHz. Whilst at f = 13.56 MHz the phase angle $\varphi \approx 90°$, at f = 27.12 MHz we obtain $|Z|$ = 17.7 Ω and $\varphi = 83.2°$, and at the resonance frequency the modulus of the impedance is $|Z|_{res}$ = 2.2 Ω. From (6) we can define a correction factor:

$$k = U_{rf}\ /U_{pr}. \quad (7)$$

At 27.12 MHz we obtain k = 3.004, i.e. the true voltage across the electrodes is three times higher than that measured by the external rf probe.

Figure 3b shows the value of the correction factor k against frequency f, obtained from formulas (6) and (7)

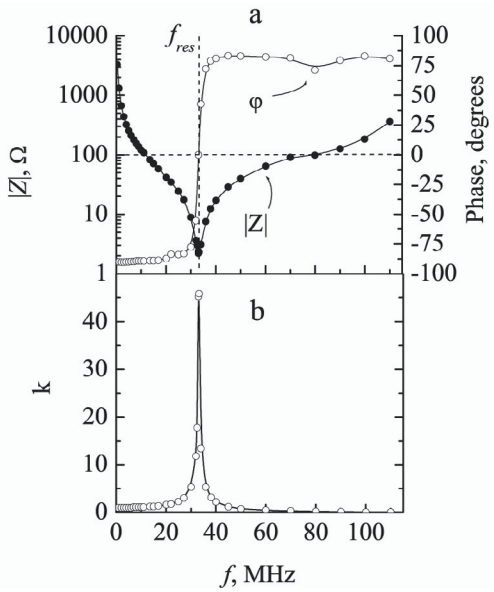

Fig. 3. (a) The impedance modulus $|Z|$ and the phase angle φ against frequency f. (b) The value of a correction factor k (7) against frequency f.

and values of $|Z|$, presented in Figure 3a. It is obvious from the figure that the quantity k possesses a clearly expressed peak at $f = f_{res}$, the correction factor approaching the value $k \approx 46$.

Now let us consider how we can use measured rf breakdown curves to estimate the voltage across the electrodes.

4 Determination of electrode voltage

The electron drift velocity can be determined, as a function of reduced electric field, from the coordinates of the turning point on the measured breakdown curves of a capacitive RF discharge [9–15]. As is known [9–16], in the low-pressure range to the left of the breakdown-curve minimum of the RF discharge one observes a region of multivalued dependence of the RF breakdown voltage U_{rf} on the gas pressure p. Figure 4 depicts the breakdown curve and the coordinates of the turning point for a spacing of 2.3 cm (at the pressure value $p = p_t$ and the rf voltage value $U_{rf} = U_t$). At the turning point, the amplitude A of the electron displacement is equal to one-half of the inter-electrode gap $A = \frac{d}{2} = \frac{V_{dr}}{\omega}$ [14–16]. The electron drift velocity V_{dr} at the turning point of the rf breakdown curve is equal to

$$V_{dr} = d\pi f. \quad (8)$$

The coordinates of the turning point allow the determination of the reduced field, E/p, corresponding to this electron drift velocity. From Figure 4 we see that the coordinates of the turning point are equal to p_t = 0.096 torr and U_t = 127 V. Then E/p = 570.9 V/(cm torr) and $V_{dr} = 9.8 \times 10^7$ cm/s. The values of the electron drift velocity determined from our measured breakdown curves

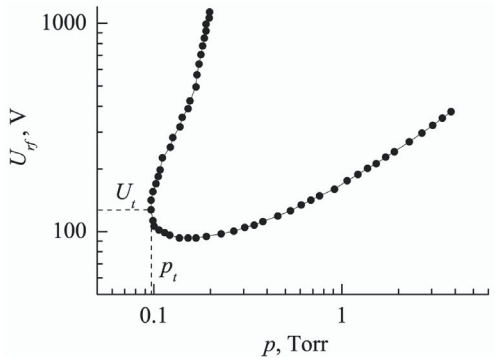

Fig. 4. Breakdown curves for the RF discharge in N_2 for $d = 2.3$ cm, $f = 13.56$ MHz.

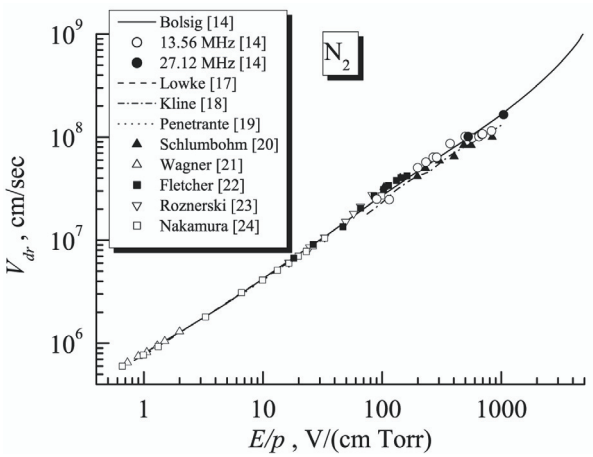

Fig. 5. The electron-drift velocity in nitrogen against E/p [14]: the solid curve presents the calculated data obtained with the Bolsig code [14], empty circles are for the experimental data from turning points ($f = 13.56$ MHz) [14], solid circles are for the experimental data from turning points ($f = 27.12$ MHz) [14], dash curve presents the calculation data from [17], dash-dot curve presents the calculation data from [18], dot curve presents the calculation data from [19], solid triangles are for the measured data from [20], empty triangles are for the experimental data from [21], solid squares are for the experimental data from [22], the empty upside-down triangles are for the experimental data from [23] and empty squares are for the experimental data from [24].

are presented in Figure 5. We published these data for the electron drift velocity in nitrogen recently [14]. The same figure shows the results of simulations [17–19] and measurements from [20–24]. We have used the Bolsig code (Kinema Research and Software) with the cross-sections from [25] in order to obtain the values of the electron drift velocity over a wide range of E/p. Figure 5 presents the values of V_{dr} calculated with the Bolsig code in the range $E/p = 1$–5000 V/(cm torr).

The determination of the pressure-voltage coordinates of the turning points in RF breakdown curves can be used as a base for a new technique for evaluating the RF potential at the driven electrode. Consider a discharge chamber with inner planar electrodes with an inter-electrode gap of d, and an RF generator with the frequency f, connected to this device through a matchbox. The chamber should be filled with a gas for which the electron drift velocity is accurately known (for example for nitrogen or oxygen [14]). Nitrogen is a good choice, as the electron drift velocity is known over a broad E/p range (see Fig. 5) and as the multi-valued region of the breakdown curve is more distinct than in argon, helium and many other gases. The rf breakdown curve $U_{rf}(p)$ is then recorded using a small gas input rate $Q = 1$–5 sccm. As the measurements are made with the rf probe situated at the feed-through, outside the discharge vessel, we actually record the breakdown as a function of $U_{pr}(p)$. In the region to the left of the breakdown curve minimum we observe a turning point for which $\mathrm{d}U_{pr}/\mathrm{d}p = \infty$ with the coordinates $p = p_t$ and $U_{pr} = U_{t.pr}$. At this point the electron drift velocity may be easily determined according to (8). For this we need to know only the width d of the inter-electrode gap and the frequency, f, of the RF field. For example, in Figure 6a we see the rf breakdown curve for nitrogen with $d = 1.19$ cm and $f = 27.12$ MHz. At the turning point the electron drift velocity is $V_{dr} = d \cdot \pi \cdot f = 1.19 \times \pi \times 27.12 \times 10^6 = 1.01 \times 10^8$ cm/s. Then from Figure 5 we determine that we require $E/p \approx 530$ V/(cm torr) for the electrons to possess in nitrogen such drift velocity (for such an estimate it is better to use the curve obtained with the Bolsig code, because it is in good agreement with the results of measurements within the total E/p range, and it permits to determine the E/p value corresponding to the given electron drift velocity with sufficient accuracy). The coordinates of the turning point for this breakdown curve are $p_t = 0.25$ torr and $U_{pr} = 113$ V. As $E = U_{rf}\ /d$ (U_{rf} is the amplitude of the rf potential at the driven electrode), then we have from the known E/p value:

$$\frac{E}{p_t} = \frac{U_{rf}}{p_t d} = 530 \text{ V/(cm torr)},$$
$$U_{rf} = 530 p_t d = 530 \times 0.25 \times 1.19 \ = \ 158.3 \text{ V}.$$

Therefore, the true correction factor between the rf voltage U_{rf} at the driven electrode and the voltage U_{pr} recorded with the RF probe outside the discharge vessel is given by

$$k = U_{rf}/U_{pr} \approx 1.4. \tag{9}$$

This is considerably smaller than the value (3.004) estimated from the circuit model. Figure 6a shows the rf breakdown curves for $d = 1.19$ cm and $f = 27.12$ MHz: recorded with the rf probe $U_{pr}(p)$ and refined with relations (7) (with the proportionality factor $k \approx 3$) and (9) (with $k \approx 1.4$). The same figure shows the breakdown curve for $f = 13.56$ MHz. It is clear from the figure that in the high pressure range the right-hand branches of the breakdown curves for $f = 13.56$ MHz and for $f = 27.12$ MHz coincide when we use a value of $k \approx 1.4$. Previous papers [26,17] have shown that the right-hand branches of breakdown curves for different frequencies will coincide at high pressure. The right-hand branches of the RF breakdown curves for other values of the inter-electrode gap were found to coincide for $f = 27.12$ MHz

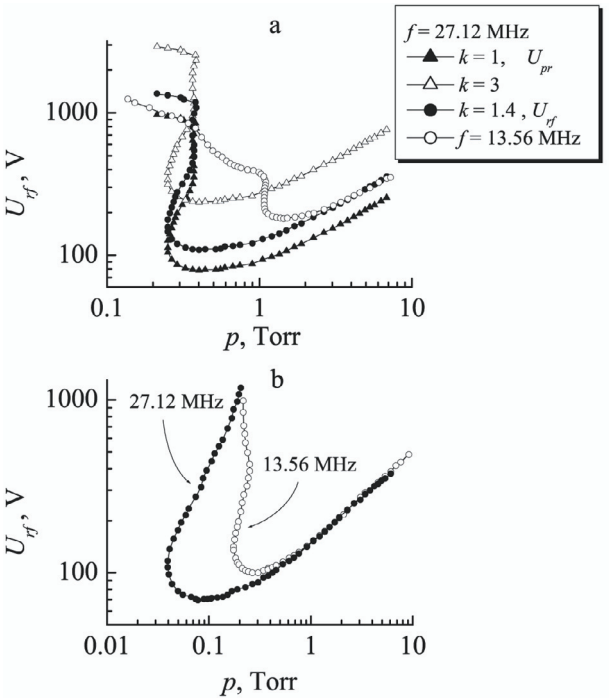

Fig. 6. (a) Breakdown curves for the RF discharge in N_2 for $d = 1.19$ cm and $f = 27.12$ MHz: recorded with the RF probe $U_{pr}(p)$ ($k = 1$) and refined with relations (7) ($k = 3$) and (9) ($k = 1.4$) and the breakdown curve for $f = 13.56$ MHz. (b) Breakdown curves for the RF discharge in N_2 for $d = 2.04$ cm, $f = 27.12$ MHz and $f = 13.56$ MHz.

and $f = 13.56$ MHz when using $k = 1.4$. Figure 6b shows the breakdown curves for $d = 2.04$ cm. The proportionality factor $k \approx 1.4$ is not valid only for nitrogen applies to all gases. Results for other gases may be found in [14], where the proportionality factor $k = 1.4$ was used for all breakdown curves for 27.12 MHz. In order to use this technique we must know accurately the gas pressure between the electrodes (and not somewhere, say, downstream in the vacuum system far from the vessel). Furthermore, the breakdown curve in the turning point region must be recorded accurately (it should be done 2–3 times and then values of the proportionality factor k should be averaged).

We have also measured the rf potential at the driven electrode directly. To do this we installed a second rf probe on top of the grounded section of the inner discharge vessel, and connected it directly to the driven electrode. We obtained the value of $k = U_{rf}/U_{pr} \approx 1.323$. This value is in much better agreement with the k value determined with our new technique compared to the value ($k = 3.004$) given by the equivalent circuit model. The insertion of the second rf probe inside the vessel undoubtedly introduces a perturbation into the impedance of the system. Therefore such "direct" recording of the rf potential is in itself not very accurate in this case but it may be used to evaluate the magnitude of U_{rf} at the driven electrode. Our new technique does not change the impedance of the discharge vessel. Furthermore, the values of the rf potential obtained with our technique and those recorded directly with the second rf probe are quite comparable. This indicates the applicability of our technique for evaluating the rf potential at the driven electrode, especially when the direct measurement is impeded.

Considerable discrepancy in the proportionality factor values obtained from the equivalent circuit model ($k \approx 3$) and from our technique ($k \approx 1.4$) may be explained by the fact that the equivalent circuit given in Figure 2 does not contain parasitic capacitances. Meanwhile, the feed-through as well as the coaxial cable possess their own capacitances, not accounted by us in the consideration, and which undoubtedly affect substantially the difference between the voltage values U_{rf} (at the driven electrode) and U_{pr} (measured with rf voltage probe).

Now let us examine which discharge chambers geometries (research and industrial) are appropriate for our technique. As it is based on recording the rf breakdown curve, the gas breakdown must be known to occur only within the gap between the planar electrodes. The inter-electrode space should be closed at the radial edge with a dielectric wall or at least with a grounded metal grid. The gap between the electrode edge and the wall (grid) should be small (not exceeding 1 mm) to prevent ignition of an RF discharge within this gap. In this case the rf breakdown curve in the low-pressure range will possess a multi-valued region with a well-expressed turning point. When planar electrodes are situated inside a large grounded vessel, or in the case of a GEC Reference Cell, at low gas pressure the breakdown occurs outside the inter-electrode space, say, between the surface of the driven electrode and the grounded wall of the large vessel. When the rf breakdown curve does not possess a turning point [28], this technique cannot be used.

Probably, the calibration factor k obtained with our technique may be inapplicable with the discharge present inside the inter-electrode gap. The impedance of the chamber filled with plasma may differ from that of the parallel-plate electrodes without the discharge. However the extinction voltage of the rf discharge we registered with the calibration factor $k = 1.4$, is in good agreement with the discharge extinction voltage determined via the well-known SIGLO-RF code (Kinema Research & Software). The extinction voltage of the rf discharge at $f = 27.12$ MHz and $p = 1$ torr, we obtained with the help of this code equals 78 V, whereas the registered value was 75 V. The authors of paper [29] claim the good agreement between the RF extinction voltages determined with the help of SIGLO-RF and registered at $f = 13.56$ MHz. Therefore we can use the calibration factor k obtained with our technique for estimating the RF voltage across the electrodes at least for the weak-current (α) mode. But for the strong-current (γ) mode the calibration factor k obtained with our technique may lead to large errors while determining the RF voltage across the electrodes. It may be stated that our technique of estimating rf voltage at the driven electrode can be applied when the discharge is absent, as well as for small discharge current values (before the discharge extinction).

5 Conclusions

Conventionally an external rf voltage probe is used for evaluating RF voltages at the driven electrode of a technological reactor that is inaccessible and direct measurements are not possible. The measurements with such a voltage probe are subject to the influence of discharge circuit elements (feed-through, cables, parasitic capacitance etc.), which may involve large errors. Therefore it is desirable to apply an auxiliary technique for estimating rf voltage values at the driven electrode that is based only on the inter-electrode gap parameters and does not depend on external circuit parameters. In this paper we propose a new technique for evaluating the rf voltage at the driven electrode based on registering the coordinates of the turning point of the rf breakdown curve in the gas for which the electron drift velocity is known in the broad E/p range. This technique allows obtaining physically reasonable rf voltage values that agree with those got from direct measurements. The proportionality factor between the voltage value recorded with an external rf voltage probe and the actual rf voltage value at the driven electrode may be used for moderate discharge current values.

References

1. W.G.M. van der Hoek, C.A.M. de Vries, M.G.J. Heijmam, J. Vac. Sci. Technol. B **5**, 647 (1987)
2. B. Andries, G. Ravel, L. Peccoud, J. Vac. Sci. Technol. A **7**, 2774 (1989)
3. J.W. Butterbaugh, L.D. Baston, H.H. Sawin, J. Vac. Sci. Technol. A **8**, 916 (1990)
4. W.C. Roth, R.N. Carlile, J.F. O'Hanlon, J. Vac. Sci. Technol. A **15**, 2930 (1997)
5. P.A. Miller, Proc. SPIE **1594**, 179 (1991)
6. P.A. Miller, H. Anderson, M.P. Splichal, J. Appl. Phys. **71**, 1171 (1992)
7. M.A. Sobolewski, J. Vac. Sci. Technol. A **10**, 3550 (1992)
8. M.A. Sobolewski, IEEE T. Plasma Sci. **23**, 1006 (1995)
9. V.A. Lisovskiy, V.D. Yegorenkov, *Record-Abstracts of IEEE International Conference on Plasma Science, San Diego, USA, 1997*, p. 137
10. V.A. Lisovskiy, Tech. Phys. Lett. **24**, 308 (1998)
11. V.A. Lisovskiy, V.D. Yegorenkov, J. Phys. D Appl. Phys. **31**, 3349 (1998)
12. V.A. Lisovskiy, V.D. Yegorenkov, J. Phys. D Appl. Phys. **32**, 2645 (1999)
13. V. Lisovskiy, S. Martins, K. Landry, D. Douai, J.-P. Booth, V. Cassagne, J. Phys. D Appl. Phys. **38**, 872 (2005)
14. V. Lisovskiy, J.-P. Booth, K. Landry, D. Douai, V. Cassagne, V. Yegorenkov, J. Phys. D Appl. Phys. **39**, 660 (2006)
15. V. Lisovskiy, J.-P. Booth, K. Landry, D. Douai, V. Cassagne, V. Yegorenkov, J. Phys. D Appl. Phys. **39**, 1866 (2006)
16. S.M. Levitskii, Sov. Phys.-Tech. Phys. **2**, 887 (1957)
17. J.J. Lowke, Aust. J. Phys. **16**, 115 (1963)
18. L.E. Kline, J.G. Siambis, Phys. Rev. A **5**, 794 (1972)
19. B.M. Penetrante, J.N. Bardsley, J. Phys. D Appl. Phys. **17**, 1971 (1984)
20. H. Schlumbohm, Z. Phys. **184**, 492 (1965)
21. E.B. Wagner, F.J. Davis, G.S. Hurst, J. Chem. Phys. **47**, 3138 (1967)
22. J. Fletcher, I.D. Reid, J. Phys. D Appl. Phys. **13**, 2275 (1980)
23. W. Roznerski, K. Leja, J. Phys. D Appl. Phys. **17**, 279 (1984)
24. Y. Nakamura, J. Phys. D Appl. Phys. **20**, 933 (1987)
25. A.V. Phelps, L.C. Pitchford, Phys. Rev. A **31**, 2932 (1985)
26. S. Githens, Phys. Rev. **57**, 822 (1940)
27. M. Chenot, Ann. Phys.-Paris **3**, 277 (1948)
28. V. Lisovskiy, S. Martins, K. Landry, D. Douai, J.-P. Booth, V. Cassagne, V. Yegorenkov, Phys. Plasmas **12**, 093505 (2005)
29. V. Lisovskiy, J.-P. Booth, S. Martins, K. Landry, D. Douai, V. Cassagne, Europhys. Lett. **71**, 407 (2005)